DOI: 10.13009/EUCASS2025-582
11TH EUROPEAN CONFERENCE FOR AERONAUTICS AND SPACE SCIENCES (EUCASS)

Theoretical Study on the Applicability of Green Propellants in RBCC Engines

Timo Gonschior⋆†, *Friedolin Strauss*⋆, *Dr. Christoph Kirchberger*⋆ *and Prof. Dr. Stefan Schlechtriem*⋆
⋆*German Aerospace Center (DLR), Institute of Space Propulsion*
Im Langen Grund
74239 Hardthausen am Kocher
Germany
timo.gonschior@dlr.de · friedolin.strauss@dlr.de
†Corresponding author

Abstract

This study estimates the implications of using so-called Green Propellants on a Rocket Based Combined Cycle's (RBCC) performance. A simplified thermodynamic engine model is implemented and propellant combinations of H_2O_2 and N_2O with light hydrocarbons as well as their monopropellant use cases are investigated regarding the overall specific impulse. The Green Propellants lead to a reduction in I_{sp} of about 10 % compared to O_2 + kerosene. This reduction can be justified by the advantages in terms of storability and handling. This study concludes that Green Propellants are a viable option for RBCCs and should be investigated further in the future.

Nomenclature

Symbols

A	cross-sectional flow area (m^2)
F_T	thrust force (N)
I_{sp}	specific impulse (s)
M	Mach number (-)
$\mathcal{M}$	molar mass (g/mol)
R	specific gas constant ($J/(kg\,K)$)
$\mathcal{R}$	universal gas constant ($J/(K\,mol)$)
T	temperature (K)
ΔT	temperature rise (K)
c_p	isobaric specific heat capacity ($J/(kg\,K)$)
g	gravitational acceleration (m/s^2)
$\dot{m}$	mass flow rate (kg/s)
p	pressure (Pa, bar)
u	flow velocity (m/s)
α	bypass ratio (-)
γ	specific heat ratio (-)
η_c	combustion efficiency (-)
σ	total pressure recovery coefficient (-)

Subscripts

0	free stream
3	combustor entry
4	combustor exit
10	main nozzle exit
c	combustion chamber
e	mixing section exit
$f2$	secondary fuel
i	station of equalized pressure
m	molar
n	mean value over main nozzle
p	primary flow (rocket exhaust)
s	secondary flow (air)
t	stagnation condition
x	placeholder for either p, s or e

Superscripts

$*$	throat

1. Introduction

Super- and hypersonic flight places challenging demands on the vehicle's propulsion system. Ramjet and scramjet based systems are the propulsion systems of choice for flight Mach numbers above 2 [1]. The airbreathing nature offers high specific impulse without the mechanical complexity and limitations at supersonic flight that come with turbojet engines. However, since they rely on the dynamic pressure for compression they are inefficient at low flight Mach numbers and cannot provide static thrust. Therefore, vehicles with this kind of engines rely on a booster stage

DOI: 10.13009/EUCASS2025-582

or a secondary propulsion system for the acceleration phase. Combined cycle engines are an approach to avoid separate booster stages and to reduce the added mass and build volume of a secondary engine by increasing the scale of integration.

The supportive propulsion system is integrated in the main flow path of the (sc)ramjet engine. In case of a Turbine Based Combined Cycle (TBCC) engine that would be a turbojet engine or a rocket driven compressor that may be bypassed at high Mach numbers [2]. The mechanically much less complex alternative are Rocket Based Combined Cycles (RBCC), in which a rocket engine is integrated in the flowpath. The rocket provides static thrust and acts as an ejector at low Mach numbers, thereby increasing the air mass flow through the engine. Due to this entrained air, the ram combustor can be used for afterburning at low Mach numbers already, hence increasing the specific impulse over that of the rocket engine alone [3]. Since they can be used from lift-off to orbit, these systems are considered to be potential candidates for future single stage to orbit (SSTO) launch systems.

RBCC engines have been studied extensively in the past. However, the technical maturity of these systems is not yet sufficient for actual technical application and further research is still necessary. Challenges exist for example in the mode transition from ejector mode to pure ramjet operation. The throttling of the rocket during the mode transition as well as the combustion organization in the secondary combustor are crucial to a stable mode transition. It was found that the flame holding characteristics of the rocket exhaust can aid the stable transition [4, 5]. Another challenge is the length of the mixing section required for complete mixing [3]. Researchers are investigating options to increase the contact surface between the rocket exhaust and the entrained air or to increase vorticity [6, 7, 8]. However, these approaches often come with their own challenges like cooling demands and increased flow resistance.

Previous research focused mostly on oxygen as oxidizer in the embedded rocket. It was paired often with hydrogen or kerosene as fuel. In the following, an overview over research activities using more unconventional fuels is given. In an experimental study Li et al. [9] used ethanol with oxygen in the gas generator of a rocket ejector in simultaneous mixing and combustion (SMC) configuration to study the effect of the ejector geometry and primary rocket chamber pressure. Dijkstra et al. [10] used ethene with air as primary propellants in an experimental setup with hydrogen as secondary fuel. The application of methane with oxygen was proposed in [11].

Jung et al. [12] used hydrogen peroxide blended with ethanol as gas generator for a ground testing facility for ramjet combustors. A rocket engine for the use in an RBCC experimental setup that uses kerosene and hydrogen peroxide as propellants was developed and tested by Miller et al. [13]. The hydrogen peroxide was decomposed catalytically and the kerosene was added to the decomposition products. A similar approach was proposed by Park et al. [14] and the corresponding rocket engine was tested experimentally. In an experimental study by Fang et al. [15], nitrous oxide with kerosene was used, specifically because a lower combustion temperature was desired in that test setup than would have been achievable with oxygen as oxidizer. In the 1970s unsymmetrical dimethylhydrazine (UDMH) was used to operate the ejector rocket in an experimental study. [16]

Additionally, some researchers studied the ejector physics using replacement gases like nitrogen [17], oxygen [7] and air [18, 19]. Studies that investigated the effects of single properties of the primary exhaust are limited so far. Jin et al. [20] examined the impact of specific heat ratio on the pressurization performance of an ejector, both experimentally and numerically. They used argon, nitrogen and carbon dioxide as replacement fluids. Han et al. [21] investigated the influence of molar mass on the ejector and engine performance theoretically. They investigated the molar masses of hydrogen, water vapor and general hydrocarbons. They concluded that a lower molar mass is beneficial for both the bypass ratio and the overall specific impulse.

Most of the RBCC research is based on conventional propellants like oxygen as oxidizer and hydrogen or kerosene as fuel. Other propellant combinations are the exception and typical "Green Propellants" have not been used in the context of rocket ejectors to the author's knowledge. However, oxygen and hydrogen have to be stored cryogenically which greatly increases complexity of the overall system. Storable propellants are favorable not only for military but also commercial applications. Kerosene on the other hand is storable but poses additional challenges like the formation of carbon deposits. Therefore, for future missions it is advisable to have a larger portfolio of options to choose from.

Green Propellants by definition offer good storability and easy handling and should therefore be included in this portfolio. At the DLR Institute of Space Propulsion in Lampoldshausen, at the department of Satellite and Orbital Propulsion, extensive research is being conducted on different types of Green Propellants [22]. In particular strong expertise has been built with propellant combinations based on hydrogen peroxide [23], nitrous oxide [24] and nitromethane [25]. As a synergy between the experience in Green Propellants and in high speed airbreathing propulsion, a research project regarding the application of Green Propellants in RBCC was recently started. The goal is to increase the understanding of the implications of primary propellant choice on the design, operation and performance of RBCCs and to gain experience with the technical realization of an RBCC with this kind of propellants. The focus will be on H_2O_2- and N_2O-based propellants. As a first step, this study estimates how these propellants, paired with light hydrocarbons and used as monopropellants, perform in an RBCC in terms of specific impulse. For that, a sim-

DOI: 10.13009/EUCASS2025-582

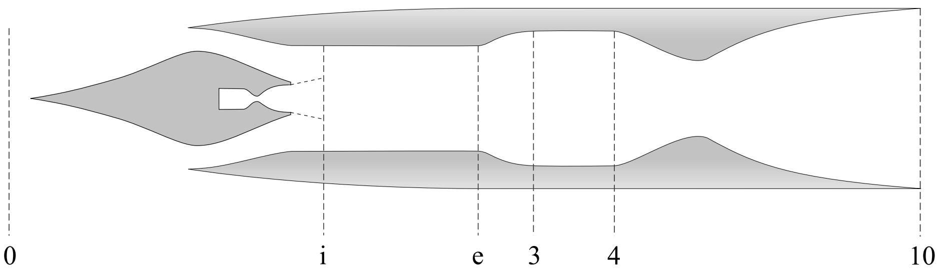

Figure 1: Schematic of the modeled ejector-ramjet engine

plified thermodynamic model is employed. The results are compared to the conventional combination of kerosene and oxygen and the previously proposed combination of kerosene and hydrogen peroxide. In the future, a more elaborate engine model will be designed for deeper insights into implications of propellant choice. This model will aid the design of an experimental RBCC model and therefore lead to a test campaign at the air vitiator facility M11.1 at DLR Lampoldshausen.

2. Method

A thermodynamic model is implemented which enables the estimation of performance parameters of an RBCC engine in ejector ramjet mode. The model is applied to different propellant combinations and various operating points in order to compare the propellants and to investigate influences of the primary exhaust properties.

2.1 Thermodynamic Engine Model

For this study only the ejector ramjet mode is regarded, therefore it is sufficient to consider a model as depicted in Figure 1. This model differs from the actual architecture that would be used for hypersonic flight mission primarily in that it has a geometrical throat behind the combustion chamber.

The model serves only as a means of estimating performance at different operating points. Complex flow phenomena are not covered by this model. The primary rocket flow is taken to be an ideal gas. It is assumed that primary and secondary flow first equalize in terms of pressure and only then start to mix. The point of equalized pressure is denoted as station i. The mixed flow is assumed to choke at the mixing section exit (station e). In reality there are numerous modes of operation for the rocket ejector with different choking modes and much more complex models would be necessary to account for that. However this kind of model is considered to be representative of the overall performance in literature [26].

The ejector model is based on a zero-dimensional control volume method. The calculation is performed iteratively. A static pressure p_i is assumed so that isentropic relations can be utilized to calculate the mass flow of primary and secondary flow. The assumption of $M_e = 1$ allows for the calculation of the mixed flow conditions at station e. The pressure p_i can than be updated based on the momentum balance between station i and e. The calculation is repeated until convergence of p_i is reached.

The ejector model was described by Han et al. [21] which was an adaptation of the model described in [26]. For the sake of completeness the equations are stated below together with the inlet and combustor calculations. This model requires the primary flow stagnation conditions p_{tp} and T_{tp} as well as the stagnation conditions p_{t0} and T_{ts} of the freestream air flow and the environmental static pressure p_0. Using the freestream Mach number M_0 and the flight altitude H as input variables, the secondary flow conditions are acquired using a standard atmosphere model and isentropic relations. The primary conditions are obtained using NASA CEA [27] with the primary oxidizer-fuel-ratio ROF_1 and the primary chamber pressure p_{cp} as additional input parameters.

The inlet total pressure loss is modeled via an empirical relation taken from [28]:

$$p_{ts} = p_{t0}\sigma \tag{1}$$

$$\sigma = 0.9945 - 0.02811M_0 - 0.0215M_0^2 + 0.0016M_0^3 \tag{2}$$

where p_{ts} is the total air pressure behind the inlet and σ the total pressure recovery coefficient.

DOI: 10.13009/EUCASS2025-582

Based on the assumed value for p_i, the Mach numbers of the primary and secondary flows at station i, M_{pi} and M_{si} can be calculated using the isentropic relations:

$$M_{pi} = \sqrt{\frac{2}{\gamma_p - 1}\left[\left(\frac{p_{tp}}{p_0}\frac{p_0}{p_i}\right)^{\frac{(\gamma_p-1)}{\gamma_p}} - 1\right]} \tag{3}$$

$$M_{si} = \sqrt{\frac{2}{\gamma_s - 1}\left[\left(\frac{p_{ts}}{p_0}\frac{p_0}{p_i}\right)^{\frac{(\gamma_s-1)}{\gamma_s}} - 1\right]} \tag{4}$$

Here, γ_p and γ_s are the specific heat ratios of the primary and secondary flow respectively. For the primary stagnation pressure p_{tp} pressure losses in the primary nozzle are neglected, so that $p_{tp} = p_{cp}$. The cross-sectional areas of the primary flow at station i, A_{pi} and A_{si} are calculated as

$$\frac{A_{pi}}{A} = \frac{A_{pi}}{A_p^*}\frac{A_p^*}{A} \tag{5}$$

and

$$\frac{A_{si}}{A} = 1 - \frac{A_{pi}}{A}. \tag{6}$$

The cross-sectional area of the primary rocket throat is denoted as A_p^*, while A is the area of the mixing section. The mass flow rates $\dot{m}_p$ and $\dot{m}_s$ of primary and secondary flow are now calculated via

$$\frac{\dot{m}_p}{A} = \sqrt{\frac{\gamma_p}{R_p T_{tp}}} p_{tp} M_{pi} \frac{A_{pi}}{A}\left(1 + \frac{\gamma_p - 1}{2} M_{pi}^2\right)^{-\frac{\gamma_p+1}{2(\gamma_p-1)}} \tag{7}$$

and

$$\frac{\dot{m}_s}{A} = \sqrt{\frac{\gamma_s}{R_s T_{ts}}} p_{ts} M_{si} \frac{A_{si}}{A}\left(1 + \frac{\gamma_s - 1}{2} M_{si}^2\right)^{-\frac{\gamma_s+1}{2(\gamma_s-1)}} \tag{8}$$

with R_p and R_s being the specific gas constants for primary and secondary flow. The bypass ratio α is then defined as

$$\alpha = \frac{\dot{m}_s}{\dot{m}_p} \tag{9}$$

The fluid properties of the mixed flow at station e, namely the mass specific isobaric heat capacity c_{p_e}, the specific heat ratio γ_e and the molar mass $\mathcal{M}_e$ can be obtained from using the bypass ratio and the respective properties of the primary and secondary flows:

$$c_{p_e} = \left(\frac{\alpha}{1+\alpha}\right) c_{p_p} + \left(\frac{1}{1+\alpha}\right) c_{p_s} \tag{10}$$

$$\gamma_e = \left(\frac{\alpha}{1+\alpha}\right) \gamma_p + \left(\frac{1}{1+\alpha}\right) \gamma_s \tag{11}$$

$$\mathcal{M}_e = \left(\frac{\alpha_m}{1+\alpha_m}\right) \mathcal{M}_p + \left(\frac{1}{1+\alpha_m}\right) \mathcal{M}_s \tag{12}$$

The molar bypass ratio α_m is defined as

$$\alpha_m = \alpha \frac{\mathcal{M}_p}{\mathcal{M}_s} \tag{13}$$

The specific gas constants are

$$R_x = \frac{\mathcal{R}}{\mathcal{M}_x} \tag{14}$$

for the respective flows, with $\mathcal{R}$ being the universal gas constant. The exit conditions are calculated using the assumption of exit choking as stated before. For the calculation of the mixed flow temperature T_e the energy conservation is applied additionally:

$$\frac{T_e}{T_{tp}} = \left(\frac{2}{\gamma_e + 1}\right) \frac{c_{p_p}}{(\alpha+1)\, c_{p_e}}\left[\alpha \frac{c_{p_s}}{c_{p_p}} \frac{T_{ts}}{T_{tp}} + 1\right] \tag{15}$$

DOI: 10.13009/EUCASS2025-582

The exit pressure p_e is calculated using the ideal gas law and, again, the assumption of $M_e = 1$:

$$\frac{p_e}{p_0} = \sqrt{\frac{\gamma_p R_e}{\gamma_e R_p}} \frac{A_p^*}{A} (1+\alpha) \frac{p_{tp}}{p_0} \sqrt{\frac{T_e}{T_{tp}}} \left(\frac{\gamma_p + 1}{2}\right)^{-\frac{\gamma_p+1}{2(\gamma_p-1)}} \tag{16}$$

The momentum balance between stations i and e offers a way of calculating p_i as follows:

$$\frac{p_i}{p_0} = \frac{p_e}{p_0} (1+\gamma_e) \left(1 + \frac{A_{si}}{A} \gamma_s M_{si}^2 + \frac{A_{pi}}{A} \gamma_p M_{pi}^2\right)^{-1} \tag{17}$$

The update scheme for p_i is also adopted from [21] as

$$\left(\frac{p_0}{p_i}\right)_{next} = f \left(\frac{p_0}{p_i}\right)_{new} + (1-f) \left(\frac{p_0}{p_i}\right)_{old} \tag{18}$$

with $f = 0.05$ as weighting factor [21]. The convergence criterion is set to a relative error of 10^{-3}. Since the cross section increases in the combustor to A_3 the Mach number in the combustor M_3 is evaluated from the Mach-area-relation

$$\frac{A_3}{A} = \frac{M_e}{M_3} \left(\frac{1 + \frac{\gamma_e-1}{2} M_3^2}{1 + \frac{\gamma_e-1}{2} M_e^2}\right)^{\frac{\gamma_e+1}{2(\gamma_e-1)}} \tag{19}$$

and the static pressure p_3 and temperature T_3 are obtained via the isentropic relations. The temperature rise ΔT is calculated using NASA CEA and the total temperature at the combustor exit T_{t4} is calculated as

$$T_{t4} = \eta_c \Delta T + T_{t3} \tag{20}$$

with the total temperature at the entry of the combustor T_{t3} and the combustion efficiency η_c, which is assumed to be 0.9 in this study, which is within the range found in literature [29]. This value depends on variables beyond the scope of this study. The ratio of secondary fuel mass flow $\dot{m}_{f2}$ to ejector mass flow $\dot{m}_e = \dot{m}_p + \dot{m}_s$ is always chosen to be the optimal ratio with regards to the overall I_{sp}. The loss in total pressure over the combustor is not considered in this model so that $p_{t4} = p_{te}$.

The nozzle is assumed to be adjustable so that it always expands ideally to atmospheric pressure p_0. Therefore the mach number at the nozzle exit M_{10} can be calculated as

$$M_{10} = \sqrt{\frac{2}{\gamma_n - 1}\left[\left(\frac{p_{t4}}{p_0}\right)^{\frac{\gamma_n-1}{\gamma_n}} - 1\right]} \tag{21}$$

with the mean specific heat ratio over the nozzle $\gamma_n = (\gamma_4 + \gamma_{10})/2$, where γ_4 and γ_{10} are taken from NASA CEA calculations. The static exit temperature T_{10} is obtained from the isentropic relation

$$T_{10} = T_{t4} \left(1 + \frac{\gamma_n - 1}{2} M_{10}^2\right)^{-1} \tag{22}$$

and the exit velocity can be calculated as

$$u_{10} = M_{10} \sqrt{\gamma_n R_n T_{10}} \tag{23}$$

with the specific gas constant of the exhaust R_n. The thrust F_T and specific impulse I_{sp} are calculated as follows:

$$F_T = \dot{m}_t u_{10} - \dot{m}_s u_0, \tag{24}$$

$$I_{sp} = \frac{F_T}{g\left(\dot{m}_p + \dot{m}_{f2}\right)} \tag{25}$$

with

$$\dot{m}_t = \dot{m}_e + \dot{m}_{f2}, \tag{26}$$

$$u_0 = M_0 \sqrt{\gamma_s R_s T_0} \tag{27}$$

and the gravitational acceleration g.

DOI: 10.13009/EUCASS2025-582

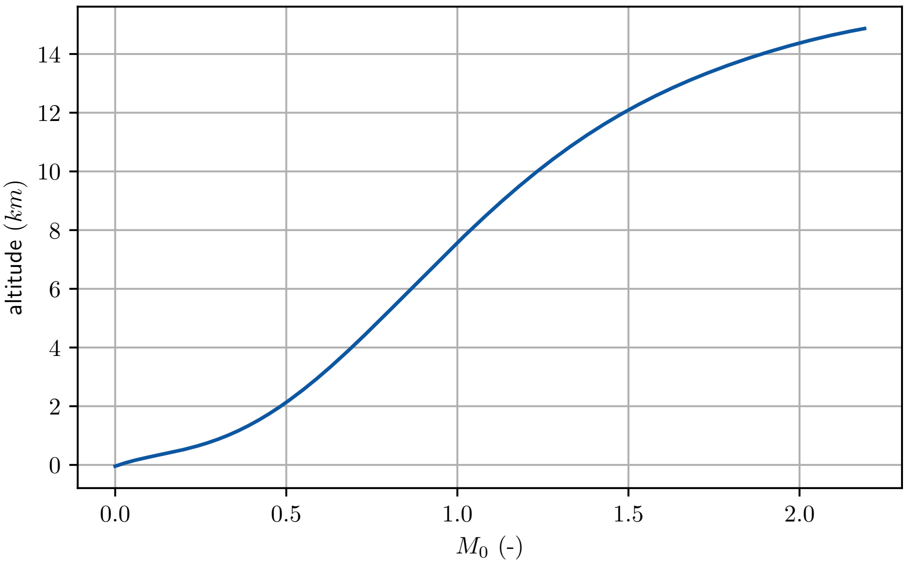

Figure 2: Trajectory of altitude vs. flight Mach number

2.2 Parameter and propellant selection

The goal of this analysis is to compare different propellant combinations in terms of overall engine performance. The effects of the molar mass and the stagnation temperature of the primary exhaust are considered as well as the impact of the exhaust composition on the secondary combustion. The influence of the variable specific heat ratio is not part of this study and needs further attention in future refinements of the model. Here, γ_p was set to a constant value of 1.2, which was found to be a representative value for the propellant combinations under investigations.

Since the ramjet mode is usually applicable above Mach 2, the flight Mach number range considered in this study of the ejector ramjet mode was $M_0 = 0$ to 2.2. For the choice of flight altitude H a trajectory from [30] was taken as a reference. It is assumed that the altitude is a function of flight Mach number M_0. The used function $H = f(M_0)$ is plotted in Figure 2 for the investigated Mach number range. The area ratio of combustor to mixing section A_c/A was chosen to be 1.2 in this study, which should only have an impact on the absolute values but not on the relative behavior of the different propellant combinations. The chamber pressure of the primary rocket was set to 10 bar.

To take advantage of the expertise in the department of Satellite and Orbital Propulsion at DLR Lampoldshausen propellant combinations based on hydrogen peroxide (H_2O_2) and nitrous oxide (N_2O) are investigated in this ongoing research endeavor. In this study both oxidizers are paired with Ethane and Ethanol to provide examples of bipropellant combinations with light hydrocarbons. Ethanol is an example of a propellant that is a liquid at 1 bar and 20 $°C$ and therefore provides good storability. Ethane on the other hand offers higher heat release during combustion but requires high pressure or low temperatures for liquification. Since for now kerosene is the most likely propellant to be used as the secondary fuel in the (sc)ramjet combustor, the combination of Jet-A and hydrogen peroxide is also taken into consideration. From a system point of view, it might be advantageous to use the same fuel for primary and secondary combustion. Furthermore, both, hydrogen peroxide and nitrous oxide, are investigated as monopropellants. As a reference the combinations of kerosene (Jet-A) with oxygen is used. As secondary fuel this study only uses Jet-A regardless of the primary propellant combination.

3. Results

Figure 3 shows the trend of the specific impulse over the primary rocket mixture ratio for the different propellants for $M_0 = 0.58$ and $A/A_p^* = 30$. It is obvious that the maximum I_{sp} always lies in the fuel-rich regime. The stoichiometric ratio lies within $ROF_1 = 4$ to 8 for the propellant combinations under investigation while the I_{sp}-peaks lie within $ROF_1 = 1$ to 3. The differences between the different propellant combinations will be examined later in this section. First, it is analyzed how the propellant properties influence the I_{sp}-trend.

DOI: 10.13009/EUCASS2025-582

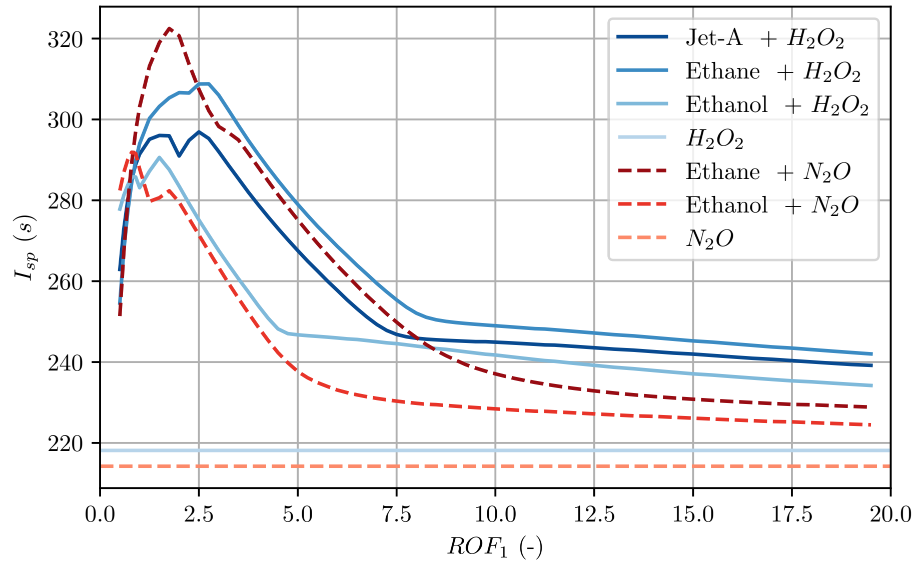

Figure 3: I_{sp}-trend over primary mixture ratio ($M_0 = 0.58,\ A/A_p^* = 30,\ p_{c1} = 10\,\text{bar}$)

3.1 Driving factors on I_{sp}

For this analysis the primary flow stagnation temperature and the molar mass of the primary exhaust are considered as well as the composition of the exhaust and its effect on the secondary combustion. Figure 4 shows the I_{sp}-trend again for ethane and hydrogen peroxide for the same conditions as in Figure 3. Each of the driving properties is considered individually in this plot, while keeping the respective other properties constant at a representative value.

It can be seen, that the influence of the primary stagnation temperature causes the specific impulse to reach its maximum at the stoichiometric ROF_1. The exhaust's molar mass and the exhaust influence on the secondary combustion cause the I_{sp} to rise and drop sharply in the fuel-rich regime. While the molar mass leads to a constant specific impulse at higher ROF_1 the influence of the exhaust composition causes the I_{sp} to rise again slightly. Each of these drivers is examined more closely in the following.

It was shown in [21] that the primary stagnation temperature has a positive effect on the ejector performance. Figure 5 demonstrates that this is also the case in the current adapted model. The left side of the figure shows the

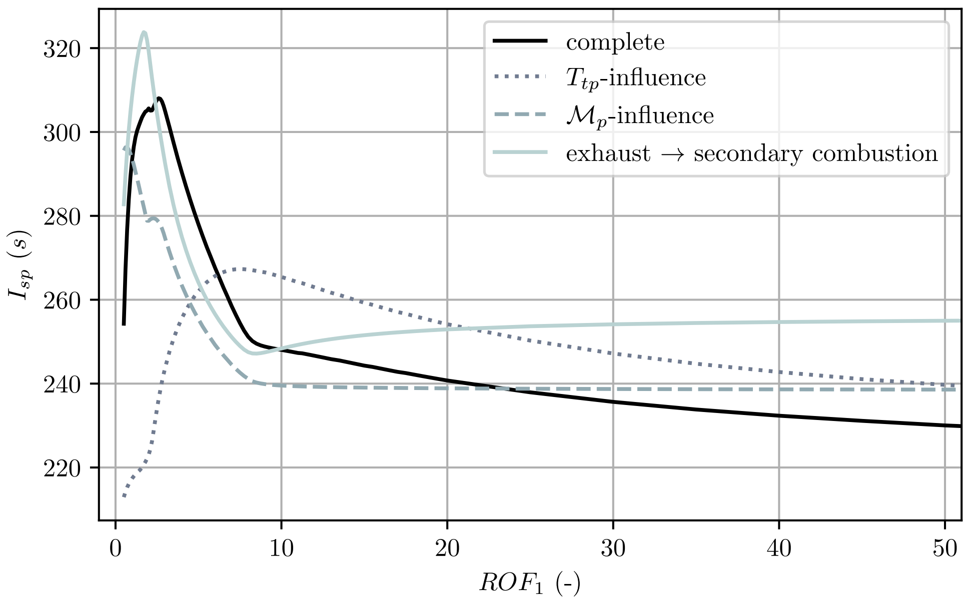

Figure 4: Influence of primary exhaust properties on I_{sp}-trend over primary mixture ratio. Example: Ethane + H_2O_2

DOI: 10.13009/EUCASS2025-582

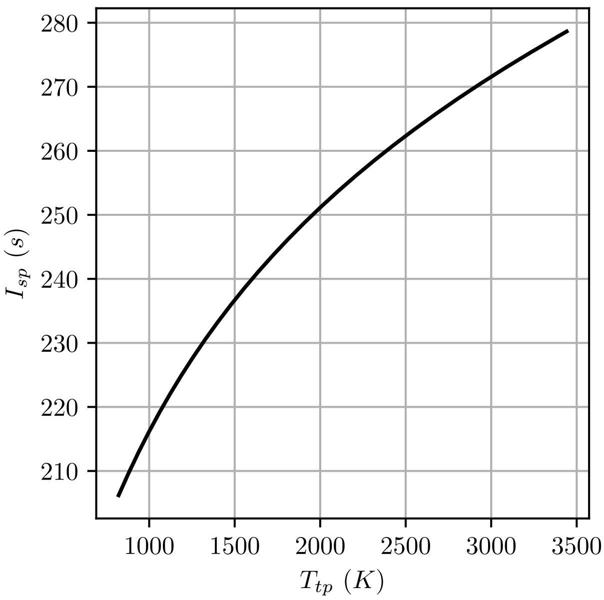

Figure 5: Influence of primary stagnation temperature on specific impulse (left), dependence of stagnation temperature on propellant combination and primary mixture ratio (right)

dependence of the total engine I_{sp} of the primary stagnation temperature when all other primary flow properties are kept constant. The stagnation temperature is highest at the stoichiometric mixture ratio as can be seen on the right of Figure 5. This explains the trend shown in Figure 4. The combinations with N_2O as oxidizers as well as the monopropellant are superior over the respective cases with H_2O_2 in regard of T_{tp}.

A higher molar mass has a negative effect on the overall I_{sp}. This effect has been described in [21] for a few replacement gases. This dependence under the assumption of otherwise constant exhaust properties is shown on the left side of Figure 6. The right side of this figure shows the molar mass of the primary exhaust as a function of primary ROF_1. Since it is assumed in the CEA equilibrium calculations that excess hydrocarbon fuel is cracked mainly into methane, hydrogen and carbon the molar mass in the fuel rich regime is low, even for Jet-A. This contributes to the peak of the specific impulse at low ROF_1. Since water vapor has a low molar mass the decomposition products of hydrogen peroxide have a lower molar mass than the products of the N_2O-decomposition, which is beneficial for the overall specific impulse.

If all properties are kept constant but the exhaust composition is allowed to change with ROF_1 this affects the combustion efficiency in the secondary combustor. This influence is shown in Figure 7. If the primary rocket runs stoichiometrically, the amount of reactive components in the exhaust are minimal, which deteriorates the secondary combustion efficiency. An excess of oxidizer in the primary rocket on the other hand enhances the secondary combustion. This explains the slight decrease in overall I_{sp} at higher ROF_1, seen in Figure 4. However, this does not explain the very prominent peak at low ROF_1. This peak is caused due to the assumption of an optimally adjusted ROF_2. During fuel-rich operation of the primary rocket much less fuel is needed in the secondary combustor to achieve stoichiometric combustion. Since the mass flow of the primary rocket stays constant over ROF_1 if all other properties are neglected, the total amount of propellant is reduced significantly. The fuel which is added in the primary rocket contributes to the air entrainment which increases the I_{sp} compared to adding the fuel only later in the secondary combustor. However, it should be noted that previous research has shown that fuel rich rocket exhaust deteriorates the overall efficiency. [31, 32] The secondary combustion partially takes place at lower pressures and the burning mixing layer affects the mixing process. Therefore, diffusion and afterburning cycles (DAB) are generally considered to be superior over simultaneous mixing and combustion cycles (SMC) [33]. This effect cannot be accounted for with the current model. The mixing itself is not modeled and it is assumed that the excess fuel in the rocket exhaust only combusts in the secondary combustor. A more elaborate model is needed to reflect these influences.

3.2 I_{sp}-comparison between the propellants

The green bipropellant combinations under investigation yielded a maximum specific impulse roughly $10 - 15\,\%$ lower than the conventional reference combination Jet-A & O_2. The comparison is shown on the left side of Figure 8. Using

DOI: 10.13009/EUCASS2025-582

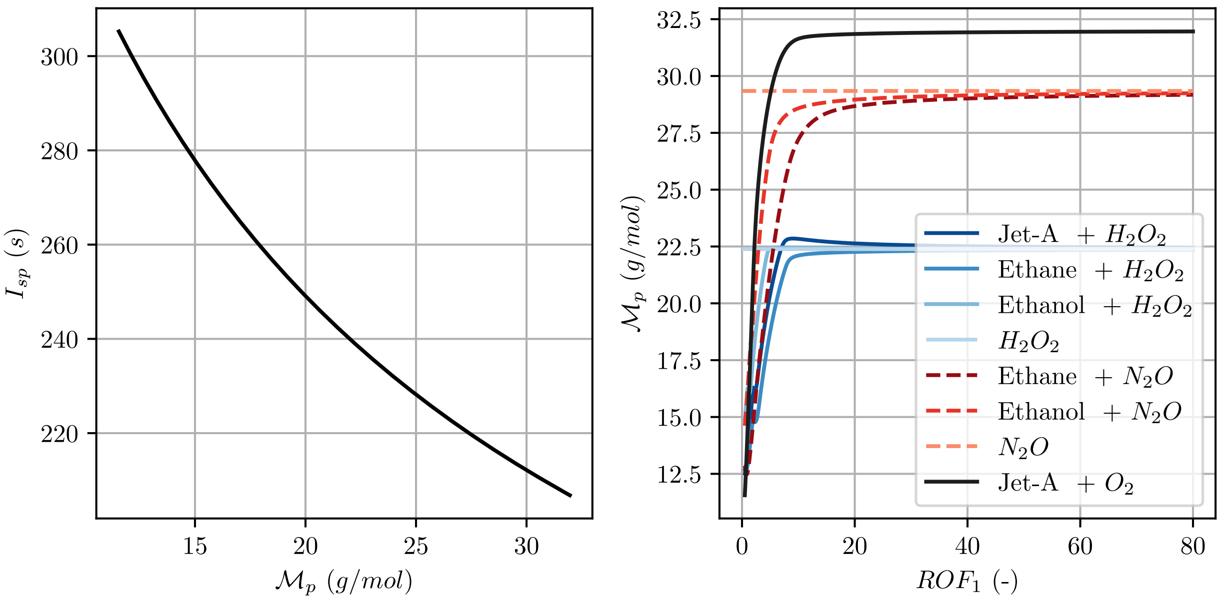

Figure 6: Influence of primary exhaust's molar mass on specific impulse (left), dependence of molar mass on propellant combination and primary mixture ratio (right)

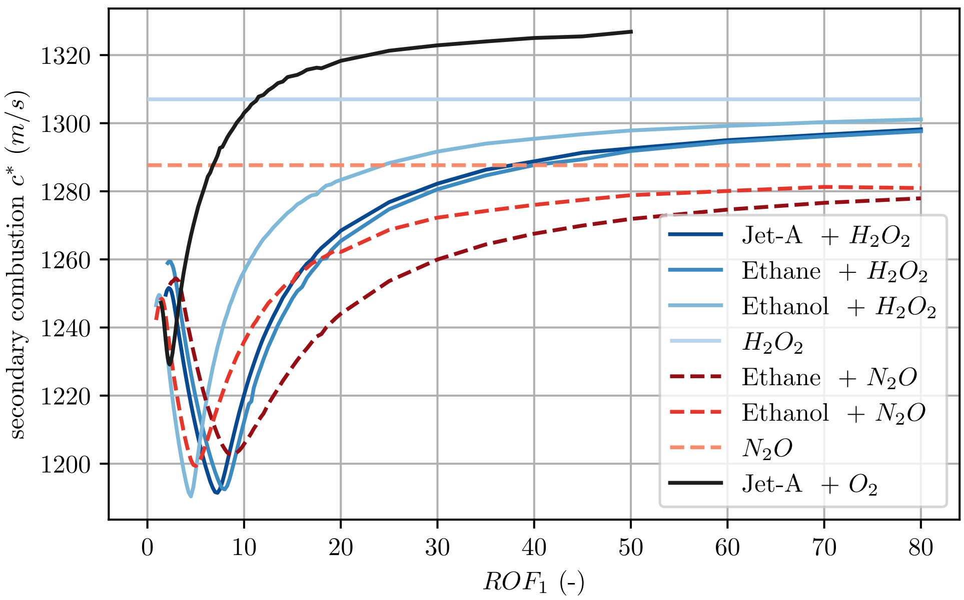

Figure 7: Influence of primary mixture ratio on secondary combustion efficiency

H_2O_2 and N_2O as monopropellants resulted in a significantly lower I_{sp} of only about 63 % of the reference I_{sp}. From this results it seems favorable to use bipropellants in fuel rich operation of the primary rocket.

However, due to the reasons stated above, fuel rich rocket exhaust has counteracting effects that decrease the overall performance, which cannot be modeled in this study. Therefore, the specific impulse is also compared for stoichiometric operation of the primary rocket. These results are shown on the right side of Figure 8. The overall I_{sp} is lowered but the relative differences between the bipropellant combinations remain similar. However, the monopropellant cases are not affected, therefore making them more competitive than in the previous consideration with an I_{sp} of now approximately 75 % of the reference case.

For each oxidizer, ethane is the fuel with the highest performance in terms of I_{sp}. Hydrogen peroxide generally leads to higher I_{sp} than nitrous oxide in combination with the same fuel. The relative performances of these propellants stay approximately the same over the studied Mach number range. This study focuses on the I_{sp} performance and mostly neglects other propellant properties that are relevant for the overall vehicle. For example, influences like density

DOI: 10.13009/EUCASS2025-582

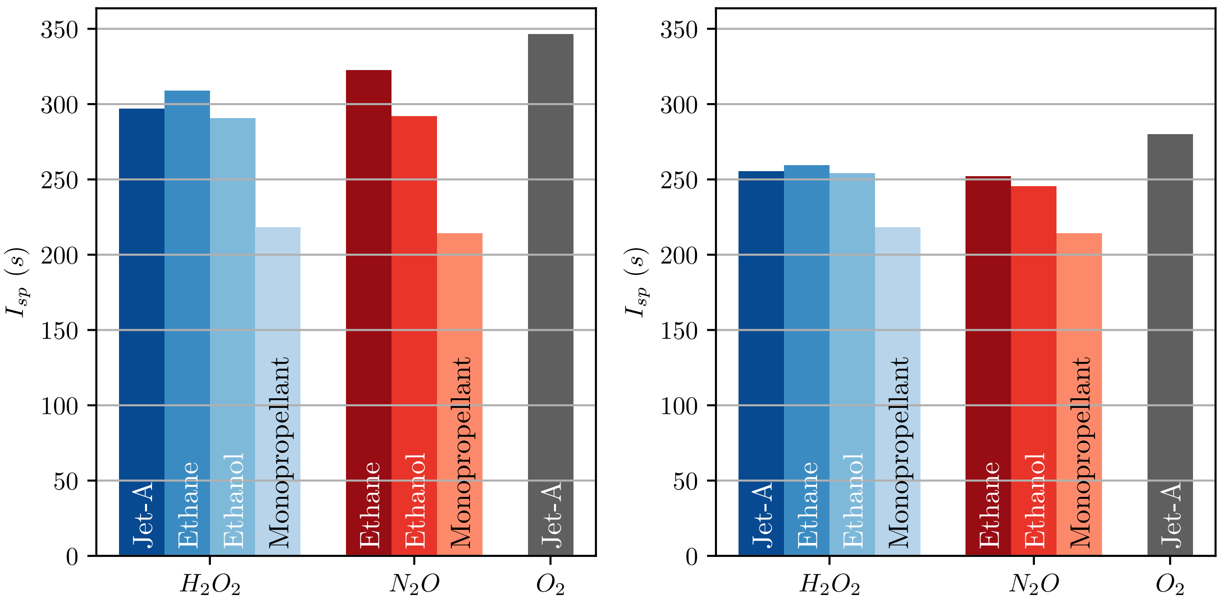

Figure 8: I_{sp}-comparison between different propellant combinations. For fuel rich optimum (left) and stoichiometric rocket operation (right)

and storability have to be taken into account as well while choosing propellants for an actual vehicle. And even though the combination of Jet-A & H_2O_2 is not the most favorable combination in terms of I_{sp}, using the secondary fuel as primary fuel could save system mass by avoiding a separate tank.

4. Conclusion and outlook

In this study a simple thermodynamic model was employed to estimate the I_{sp}-performance of green propellant combinations based on hydrogen peroxide and nitrous oxide for a rocket based combined cycle (RBCC). The influence of primary exhaust properties on the overall I_{sp} were investigated over different primary mixture ratios. In general, a low molar mass of the exhaust and a high combustion temperature are favorable for the total I_{sp}. Under the assumption of complete decomposition of the fuel into light hydrocarbons, carbon and hydrogen, a fuel rich primary rocket operation leads to lower molar mass. In general, using hydrogen peroxide leads to lower molar mass than nitrous oxide. From a point of combustion temperature, a stoichiometric operation is favorable. Nitrous oxide generally leads to higher stagnation temperatures in the primary exhaust. The secondary combustion benefits from an oxygen rich exhaust.

In general, propellants that lead to an exhaust with low molar mass and high temperature are favorable. In the case of the studied combinations, the model predicts slightly better performance for H_2O_2-based combinations than for N_2O-based ones, even though H_2O_2 leads to lower stagnation temperatures. This fact makes hydrogen peroxide additionally attractive since lower temperatures a favorable from a mechanical and material point of view.

The results of this model imply that the primary rocket should be operated in the fuel rich regime. While it makes sense that the fuel mass flow which is added in the primary rocket supports the entrainment of air, it is found in literature that fuel rich exhaust leads to degradation of the overall performance. This is only one of the aspects, the current model does not cover. A more elaborate model is required for a more detailed analysis. The coupling of combustor backpressure and the ejector was not considered. Only the exit choking mode of the ejector was taken into account. This model also does not depend on the mixer length and just assumes perfectly mixed flow at the exit. For a more extensive investigation on the implications of propellant choice on the RBCC operation a partially numerical model is being implemented that is supposed to overcome many of the shortcomings of the current study in the future. This model will also serve as a tool to help with the design of an experimental combustor as well as to define operating points of interest for the experimental test campaign.

This study only serves as a general assessment of the applicability of green propellants in rocket based combined cycles. The results show that while the I_{sp} is lower than for conventional propellants, the deterioration is not very prominent. The reduced performance therefore can potentially be justified by system implications like the enhanced storability compared to cryogenic oxygen. Additionally, the green propellants under investigation offer a higher specific impulse in the lean operation compared to combinations with pure oxygen, since the decomposition of H_2O_2 and N_2O

DOI: 10.13009/EUCASS2025-582

itself releases energy. Therefore, future research will deal with investigating the potential benefits of oxygen-rich exhaust, e.g. for flame stabilization and mode transition from ejector to ramjet operation. As a first step in the research ambitions regarding Green Propellants in RBCCs, this study shows promising results that are encouraging to continue this path of research. After a more in-depth theoretical analysis, experimental test campaigns at the air vitiator test bench M11.1 at DLR's Institute of Space Propulsion are therefore planned.

References

[1] V. Babu. *Fundamentals of Propulsion*. Springer Cham, Cham, Switzerland, 2022.

[2] R. S. Fry. A century of ramjet propulsion technology evolution. *Journal of Propulsion and Power*, 20(1):27–58, 2004.

[3] R. Daines and C. Segal. Combined rocket and airbreathing propulsion systems for space-launch applications. *Journal of Propulsion and Power*, 14(5):605–612, 1998.

[4] L Shi, G. Zhao, Y. Yang, F. Qin, X. Wei, and G. He. Experimental study on ejector-to-ramjet mode transition in a divergent kerosene-fueled rbcc combustor with low total temperature inflow. *Aerospace Science and Technology*, 99, 2020.

[5] Y. Hu, Y. Liu, Y. Wang, B. Zhou, X. Zheng, and R. Xue. Effect of the heat release on ejector-to-ramjet dynamic mode transition process in the rocket-based combined cycle engine. *International Communications in Heat and Mass Transfer*, 140, 2023.

[6] W. Escher and R. Schnurstein. A retrospective on early cryogenic primary rocket subsystem designs as integrated into rocket-based combined-cycle (rbcc) engines. In *29th Joint Propulsion Conference and Exhibit*, 1993.

[7] J. Etele, M. Kodera, and S. Ueda. Experiments with ejector rocket entrainment. *Journal of Propulsion and Power*, 32(5):1110–1118, 2016.

[8] H. Chao, Y. Huanli, and D. Jian. Mixing and combustion augmentation of the rbcc with different mixer configurations in ejector mode. *Acta Astronautica*, 174:281–293, 2020.

[9] Y. Li, G. He, and P. Liu. Experimental investigation of rocket ejector in smc combustion mode. In *42nd AIAA/ASME/SAE/ASEE Joint Propulsion Conference Exhibit*. AIAA, 2006.

[10] F. Dijkstra, A. Maree, M. Caporicci, and H. Immich. Experimental investigation of the thrust enhancement potential of ejector rockets. In *33rd Joint Propulsion Conference and Exhibit*, 1997.

[11] V.I. Timoshenko, I.S. Belotserkovets, Y.V. Knyshenko, and Y.G. Lyashenko. Hypersonic methan rocket-ramjet engines for rlv. In *55th International Astronautical Congress*, 2004.

[12] W. Jung and S. Baek. Demonstration of ethanol-blended hydrogen peroxide gas generator for ramjet combustor flow simulation. *Journal of Propulsion and Power*, 34(3), 2018.

[13] K. J. Miller, J. C. Sisco, B. L. Austin, and T. N. Martin III andW. E. Anderson. Design and ground testing of a hydrogen peroxide /kerosene combustor for rbcc application. In *39th AIAA/ASME/SAE/ASEE Joint Propulsion Conference and Exhibit*, 2003.

[14] G. Park, H. Lim, and S. Kwon. Novel ramjet propulsion system with h2o2-kerosene rocket as an initial accelerator. In *44th AIAA/ASME/SAE/ASEE Joint Propulsion Conference and Exhibit*, 2008.

[15] G. Fang, Z. Wei, Z. Wu, R. Du, and N. Wang. Experimental and numerical investigation of an embedded rocket ramjet combustor. *Acta Astronautica*, 165:105–116, 2019.

[16] J.G.Bendot, W.G. Harkins, and T.G. Piercy. Low cost hypermixing ejector ramjet program. Technical Report ARL 75-0219, Aerospace Research Laboratories, Ohio, 1975.

[17] S. Aoki, J. Lee, G. Masuya, T. Kanda, K. Kudo, and A. Murakami. Experimental investigation of an ejector-jet. In *41st Aerospace Sciences Meeting and Exhibit*. AIAA, 2003.

[18] G. Park and S. Kwon. Thrust characteristics of axi-symmetric annular bell type ejector-jets. In *43rd AIAA/ASME/SAE/ASEE Joint Propulsion Conference & Exhibit*, 2007.

DOI: 10.13009/EUCASS2025-582

[19] O. Lamberts, P. Chatelain, and Y. Bartosiewicz. Numerical and experimental evidence of the fabri-choking in a supersonic ejector. *International Journal of Heat and Fluid Flow*, 69:194–209, 2018.

[20] J. Jin, S. Kwon, and S. Kim. The affects of melecular properties of motive gas on supersonic ejection. *KSAS International Journal*, 9:98–106, 2008.

[21] S. Han, J. Peddieson Jr., and D. Gregory. Ejector primary flow molecular weight effects in an ejector-ram rocket engine. *Journal of Propulsion and Power*, 18(3):592–599, 2002.

[22] L. Werling, D. Freudenmann, S.C. Ricker, M. Wilhelm, F. Lauck, F. Strauss, K. Manassis, M. Kurilov, A. Petrarolo, T. Hörger, M. Negri, and C. Kirchberger. Research and test activities on advanced rocket propellants at dlr's institute of space propulsion in lampoldshausen. In *9th European Conference for Aeronautics and Space Sciences (EUCASS)*, 2022.

[23] M. Negri and L. Werling. Hot firing tests of a novel green hypergolic propellant in a thruster. *Journal of Propulsion and Power*, 38(3):467–477, 2022.

[24] M. Negri, L. Werling, F. Lauck, E. Goos, J. Wischek, Y. Besel, and F. Valencia-Bel. High performance propellant development - overview of development activities regarding premixed, green n2o/c2h6 monopropellants. In *Space Propulsion Conference 2022*, 2022.

[25] M. Kurilov, L. Werling, C. Kirchberger, H. Ciezki, and S. Schlechtriem. Combustion behavior of nmp-001, a nitromethane-based green rocket propellant. *Acta Astronautica*, 223:1–14, 2024.

[26] W. H. Heiser and D. T. Pratt. *Hypersonic Airbreathing Propulsion*. AIAA Education Series. AIAA, Washington DC, 1994.

[27] S. Gordon and B. J. McBride. Computer program for calculation of complex chemical equilibrium compositions and applications. *NASA Reference Publication 1311*, 1996.

[28] F. Luo, Z. Qu, Y. Long, W. Chen, J. Hou, and B. Wei. Thermodynamic performance modeling, optimization and numerical simulation of rbcc ejector mode. *Propulsion and Power Research*, 13(2):207–232, 2024.

[29] X. Wu and Z. Wei. Comparison of dual-combustion ramjet and scramjet performances considering combustion efficiency. *Applied Sciences*, 13(1):480, 2023.

[30] J. E. Bradford and J. R. Olds. Concept assessment of a hydrocarbon fueled rbcc-powered military spaceplane. *SpaceWorks Engineering, Inc.*, 2007.

[31] L. Shi, G Zhao, Y. Yang, D. Gao, F. Qin, X. Wei, and G. He. Research progress on ejector mode of rocket-based combined-cycle engines. *Progress in Aerospace Sciences*, 107:30–62, 2019.

[32] J. Chen, M. Sun, P. Li, B. An, R. Gu, M. Li, and J. Wang. Experimental and numerical study on rbcc engines performance in simultaneous and combustion cycle. *International Communications in Heat and Mass Transfer*, 150, 2024.

[33] C. Segal. Propulsion systems for hypersonic flight. *RTO-EN-AVT-116*, 2004.